Renal amyloidosis revisited: amyloid distribution, dynamics and biochemical type

Helmut Hopfer[1], Thorsten Wiech[2] and Michael J. Mihatsch[1]

[1]Pathology, University Hospital Basel, Basel, Switzerland and [2]Institute of Pathology, University Hospital Freiburg, Freiburg, Germany

Correspondence and offprint requests to: Helmut Hopfer; E-mail: hhopfer@uhbs.ch

Abstract

Background. Renal amyloidosis results from protein misfolding and leads to progressive renal insufficiency. Few data are available concerning the relevance of the histomorphological patterns and the dynamics of the disease process.

Methods. Cases of renal amyloidosis in native kidney biopsies ($n = 203$) were retrospectively evaluated for the pattern of amyloid distribution, the extent of glomerular amyloid deposition and the amount of interstitial fibrosis and tubular atrophy. One hundred and fifty-eight cases were characterized by immunohistochemistry to determine the biochemical amyloid type. Morphological findings were correlated with available clinical data.

Results. According to the predominant site of amyloid deposition, 84.6% showed a glomerular, 9.4% a vascular and 6% a tubulointerstitial distribution pattern. Within the glomeruli, amyloid was initially deposited in a focal segmental fashion that became diffuse and global in later stages. Most cases were identified as AL lambda (84/158) or AA (68/158). There was no correlation between the biochemical type and the distribution pattern. Serum creatinine correlated well with interstitial fibrosis and tubular atrophy and proteinuria with the glomerular amyloid load.

Conclusions. The relevance of the different distribution patterns is unclear at the moment, but they may be due to the physicochemical properties of the amyloid fibrils in a given patient. This may become important in future antifibrillar therapies.

Keywords: amyloidosis; immunohistochemistry; kidney biopsy; renal pathology

Introduction

Renal amyloidosis is a well-known and well-described disease, and in most cases a straightforward diagnosis for renal pathologists evaluating the kidney biopsy. The use of special stains (i.e. Congo red with polarized light or fluorescence) establishes the diagnosis without doubt. Its pathology is determined by the extracellular deposition of amyloid fibrils that assemble from instable precursor

proteins. Biochemical typing, usually performed by immunohistochemistry, establishes the biochemical type that is currently considered the key information provided by the pathologists because it determines clinical management and therapy [1–3]. In most published series from the Western world, AL amyloidosis comprises the majority of cases followed by AA amyloidosis. All other forms are only infrequently found [3, 4].

Renal amyloidosis shows a number of different distribution patterns within the kidney compartments. Although this has been described in a number of case reports and some biopsy series, these patterns have only been insufficiently characterized [5–9]. The reason for the preferential localization to one or the other compartment is not well established. It seems very likely that the varying chemicophysical properties of the amyloid fibrils determine the tropism. These result from the biochemical type, amino acid sequence and proteolytic fragmentation of the precursor proteins and/or the fibrils [1, 10–12]. Currently, the distribution patterns do not aid in the management of the patients. A number of new therapies are being developed for amyloidosis therapy. These target the formation or stability of the fibrils or aim to stabilize the precursor proteins [1].

In our study, we aimed to better describe the amyloid distribution patterns in a large series of kidney biopsies and to identify morphological parameters that may be useful for patient management, especially in the context of the emerging anti-fibrillar therapies.

Materials and methods

Study design, patients and material

Two hundred and three cases of renal amyloidosis diagnosed in native kidney biopsies between 1960 and 2007 at the Institute of Pathology were retrieved from the archives and the clinical data provided at the time of biopsy were evaluated. The study was approved by the local ethical committee.

For each patient, the following data given at the time of biopsy were recorded: age, sex, basic disease, serum creatinine and proteinuria. Most of the patients included in this study ($n = 152$) were part of a recent study on the biochemical typing of renal amyloidosis [3].

Histology

Paraffin sections stained with Periodic acid-Schiff (PAS), hemotoxylin and eosin, trichrome, methenamine silver and Congo red were reevaluated. In all cases, the number of glomeruli, obsolescent glomeruli, obsolescent glomeruli due to amyloid and glomerular crescents were counted. Sections were systematically evaluated for the presence of amyloid in the glomeruli, preglomerular arterioles, interlobular arteries, vasa recta, tubular basement membranes and interstitium. The glomerular amyloid load was scored as segmental (involving <50% of a glomerular cross section) or global ($\geq$50% of a glomerular cross section), the latter as mild/moderate or severe in the most severely affected glomerulus. The amount of interstitial fibrosis was estimated as area% of the renal cortex. The amount of interstitial inflammation was scored semiquantitatively (0 = none, 1 = minimal, 2 = mild, 3 = moderate and 4 = severe).

The biochemical type of amyloid has been determined by immunohistochemistry in all biopsies received since 1988 ($n = 158$). The amyloid-specific antibodies used in this study were a generous gift of Prof. R. Linke (Martinsried, Germany). Antibodies against AA, AL-lambda, AL-kappa and ATTR (transthyretin) were routinely employed on paraffin sections using pretreatment and the ABC method as specified by Prof. Linke [2].

Transmission electron microscopy was performed in most cases according to the standard procedures.

Statistical analysis

Differences between multiple groups were compared using the Kruskal–Wallis test and followed by a Mann–Whitney *U*-test to compare two groups with each other. Nonparametric correlation tests (Spearman's) were used where appropriate. All statistics were performed using Graph-Pad Prism version 5.01 (GraphPad Software, San Diego, CA).

Results

Patient characteristics

The age range of the patients studied was 6.7–87.2 years with a median of 59.5 years. The male to female ratio was 1.23:1. The median age of patients presenting with AA amyloidosis was slightly younger than that of the patients with AL amyloidosis [median 59.3 years (range 6.7–86.2) versus 64 years (range 41–84); $P < 0.01$]. AL amyloidosis was rare before the age of 50 (7/84 patients) and there was no case before the age of 40. There were no age or sex differences in regard to the amyloid distribution within the kidneys.

Of the 68 patients diagnosed immunohistochemically with AA-type amyloidosis, 29 (42.6%) had a clinically history of chronic (autoimmune) inflammatory disease, 8 (11.8%) of chronic infection, 5 (7.4%) of familial Mediterranean fever and 4 patients had a known malignancy (Table 1). No information was available in the other cases. Interestingly, five of the patients in the AA group also had a monoclonal gammopathy. In addition, there was one patient showing both AA and AL amyloid, who had a history of both chronic polyarthritis and monoclonal IgG.

In most of the 84 patients diagnosed with AL-type amyloidosis, no clinical history of lymphoma or monoclonal gammopathy was given. Twenty-four patients (28.6%) had plasma cell myeloma or another lymphoma and 14 (16.7%) had a known monoclonal gammopathy with a clinical diagnosis of monoclonal gammopathy of unknown significance.

Table 1. Known primary diseases provided at the time of kidney biopsy for AA and AL amyloidosis

AA amyloidosis		
Chronic (autoimmune) inflammatory disease	29/68	42.6%
Rheumatoid arthritis	15/68	
Ankylosing spondylitis	4/68	
Inflammatory bowel disease	5/68	
Others[a]	5/68	
Chronic infections	8/68	11.8%
Familial Mediterranean fever	5/68	7.4%
Known malignancy[b]	4/68	5.9%
No information provided	22/68	32.4%
AL amyloidosis		
Plasma cell myeloma	22/84	26.2%
Other B-cell non-Hodgkin lymphoma	2/84	2.4%
Paraproteinemia or paraproteinuria	14/84	16.7%
Solid malignancies[c]	1/84	1.2%
Primary myelofibrosis	1/84	1.2%
No information provided	41/84	48.8%

[a]Psoriasis (two patients), systemic lupus erythematodes, polymyalgia rheumatica and unclassified chronic autoimmune disease.
[b]Plasma cell myeloma (two patients), Morbus Waldenstrom and endometrial carcinoma.
[c]Colon cancer.

Table 2. Summary of patients <40 years of age at the time of diagnosis[a]

Age	Sex	Clinical history	Year of biopsy
6.7	Female	Juvenile rheumatoid arthritis	1994
12.0	Female	Familial Mediterranean fever	2005
15.6	*Female*	*Cystic fibrosis*	*1984*
17.5	Female	Familial Mediterranean fever	2005
19.0	Female	Not provided	1996
20.8	Female	Familial Mediterranean fever	1988
21.0	Male	Chronic autoimmune disease, unclassified	2003
22.0	Female	Rheumatoid arthritis	1993
22.6	*Male*	*Osteomyelitis*	*1964*
24.0	Male	Ankylosing spondylitis/familial Mediterranean fever	2004
24.7	*Female*	*Colitis ulcerosa*	*1982*
26.2	*Female*	*Autoimmune hemolytic anaemia*	*1981*
28.4	*Female*	*Not provided*	*1964*
29.0	*Female*	*Juvenile rheumatoid arthritis*	*1984*
29.2	*Female*	*Not provided*	*1975*
31.0	Male	Not provided	2001
31.0	Male	Rheumatoid arthritis	2001
32.0	Female	Osteomyelitis, abscesses, HIV infection	2007
33.1	*Male*	*Abscesses*	*1983*
34.6	Male	Colitis ulcerosa	1994
38.1	Female	Tuberculosis	1998
38.3	*Male*	*Osteomyelitis*	*1965*
39.0	Male	Morbus Crohn	1991

[a]All cases typed by immunohistochemistry had AA amyloidosis (patients presented in italics were not typed by immunohistochemistry).

Twenty-three patients in our study were <40 years at the time of renal biopsy. Immunohistochemical typing was performed in 14 cases. All were of the AA type (for further details see Table 2).

Biochemical type of amyloid

Immunohistochemical typing of amyloid was routinely performed in all biopsies since 1988 ($n = 158$; Figure 1A–D). Eighty-four cases (53.2%) were classified as AL, the majority [74 (88.1%)] being AL lambda. There were 10 cases with AL kappa. AA-type amyloidosis was found in 68 cases (43%). One case was both positive for AA and AL lambda. Only one case was identified as ATTR (transthyretin). Four cases were unclassifiable with the antibody panel employed (2.5%). There was insufficient biopsy material to perform immunohistochemistry for additional amyloid types in three of four cases. The remaining case was also negative for AFib, AApoA1 and ALysozyme, as well as IgA, IgG and IgM.

Distribution of amyloid

The majority of cases (170; 84.6%) had dominant glomerular amyloid deposition (glomerular type; Figure 1E and F). In 19 cases (9.4%), amyloid was found primarily in the arteries and arterioles (vascular type; Figure 1G) and in 15 cases (6%), the amyloid was mainly seen in the interstitium (interstitial type; Figure 1H). Although all cases showed dominant deposition of amyloid in one of the compartments, amyloid deposition in most cases was not limited to this compartment (see below).

Glomerular pattern and dynamics of glomerular amyloid deposition

In the glomerular type, amyloid deposits were dominantly located in the glomeruli in a focal segmental, diffuse segmental or diffuse global fashion. In most cases, there was mesangial involvement and in later stages (see below) also involvement of the peripheral capillaries (Figure 2). Due to the large number of cases, the dynamics of glomerular amyloid deposition could be investigated. The dynamics can be deduced from both the amyloid amount and distribution within a single glomerulus, the number of glomeruli involved and the presence of amyloid in the other compartments. Amyloid deposition began in a focal and segmental fashion and was involving the mesangium first (Stage I, Figure 3). As the disease progressed, the amount of glomerular amyloid increased and there was also deposition along the peripheral capillaries. It was first distributed in a diffuse segmental (Stage II) and then in a diffuse global fashion (Stage III). In the early global phase, there was a mild-to-moderate widening of the mesangium and the glomerular capillaries were still easily recognizable (Stage IIIa). The late global phase was characterized by severe mesangial as well as peripheral amyloid deposits and the number of cells within the lesions decreased. The peripheral capillaries became narrow and were less well recognizable (Stage IIIb). Finally, the glomeruli became obsolescent.

Additional, less conspicuous amyloid deposits in the arterioles were present in 50% of cases with focal segmental glomerular amyloid deposits (Figure 3; Stage I), whereas involvement of arteries and the interstitium was only present in 4.5 and 13.8%, respectively. Once the glomerular involvement was diffuse (Stage II), the majority of cases had arteriolar involvement (87.8%) and the number of cases with additional arterial and/or interstitial involvement increased. With diffuse and global glomerular amyloid deposits (Stage III), almost all cases showed arteriolar involvement and approximately two-thirds had arterial and/or interstitial involvement. Regarding the interstitial involvement, there was no predictable pattern determining involvement of tubular basement membranes or vasa recta.

Besides this common pattern of amyloid distribution, there were five cases with a diffuse nodular pattern and four cases with an evenly minimal diffuse and global amyloid distribution within the mesangium (Figure 1I and J). Focal crescents were present in four cases, but there were no other unique findings.

Vascular pattern

In the vascular type, the most obvious amyloid deposits were seen within arteries or arterioles (Figure 1G). The distribution could be segmental or circular, the first being mostly present in arcuate arteries and the later in interlobular arteries and arterioles. Most cases showed involvement of the outer media, sometimes accompanied by amyloid deposition in the adjacent interstitium. Few cases had transmural amyloid deposits, sometimes resulting in the formation of aneurysms (Figure 1K). Once the subendothelial space was involved, there was a concentric intimal fibrosis
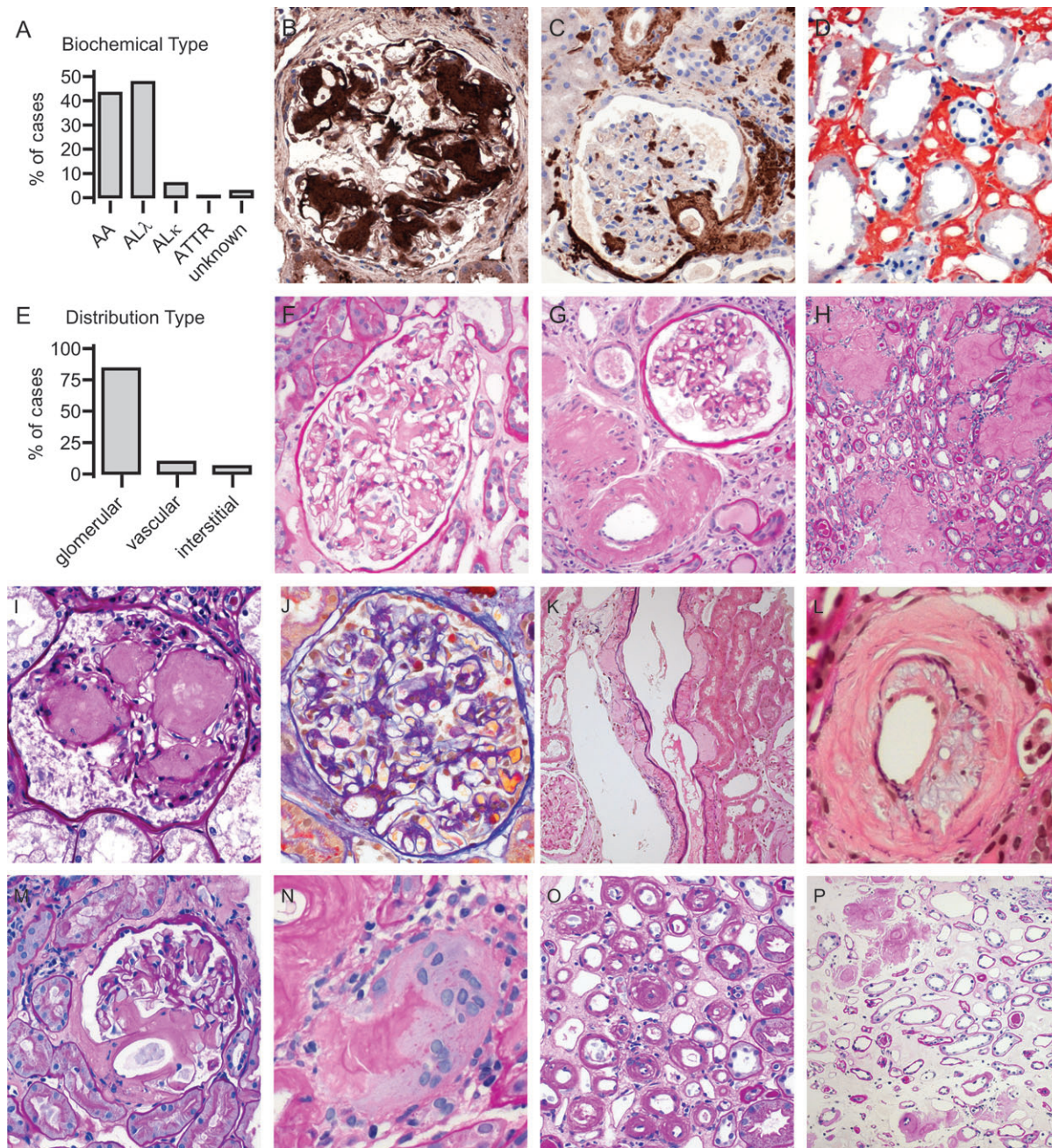
Fig. 1. (**A**) Biochemical amyloidosis types characterized by immunohistochemistry using amyloid-specific antibodies. (**B**) Glomerular amyloid deposits of the AA type (immunohistochemistry, original magnification: ×400). (**C**) Vascular, glomerular and interstitial amyloid deposits of the AL-type lambda (immunohistochemistry, original magnification: ×200). (**D**) Interstitial amyloid deposits of the AL-type kappa (immunohistochemistry, original magnification: ×400). (**E**) Distribution types of renal amyloidosis. (**F**) Glomerular type with segmental mesangial amyloid deposits (PAS, original magnification: ×400). (**G**) Vascular type with prominent amyloid deposits in an interlobular artery without glomerular involvement (PAS, original magnification: ×100). (**H**) Interstitial type affecting the medulla (PAS, original magnification: ×100). (**I**) Glomerulus with nodular amyloid deposits resembling diabetic glomerulosclerosis (PAS, original magnification: ×400). (**J**) Glomerulus with minimal global mesangial amyloid deposits (Acid Fuchsin Orange G, original magnification: ×400). (**K**) Segmental transmural amyloid deposits in an interlobular artery with formation of aneurysms (Elastica van Gieson, original magnification: ×100). (**L**) Circumferential amyloid deposits in a medium-sized interlobular artery with intimal fibrosis, stenosis and foam cells (Elastica van Gieson, original magnification: ×400). (**M**) Prominent amyloid deposits at the vascular pole of a glomerulus (PAS, original magnification: ×400). (**N**) Giant cell adjacent to amyloid in the adventitia of a small interlobular artery (PAS, original magnification: ×400). (**O**) Amyloid deposits along the vasa recta and tubular basement membranes in the medulla (PAS, original magnification: ×400). (**P**) Focal nodular amyloid deposits in the medulla (PAS, original magnification: ×200).

without elastosis and subsequent stenosis (Figure 1L) or even occlusion of the vascular lumina.

All vascular-type cases also showed glomerular amyloid deposits. These were very minute in 9/19 cases, be-coming apparent only by immunohistochemistry. The other cases showed mild to moderate glomerular involvement. In some cases, there were glomeruli with prominent amyloid deposits at the vascular pole (Figure 1M). In one
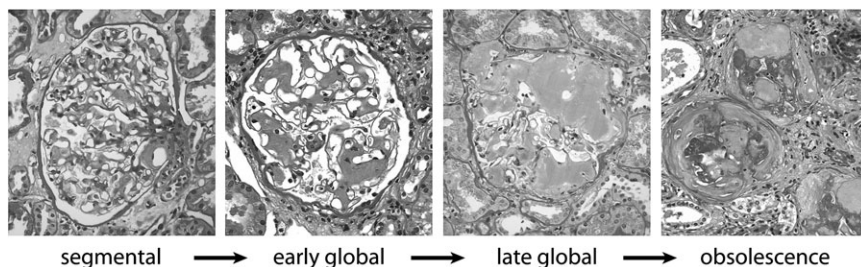
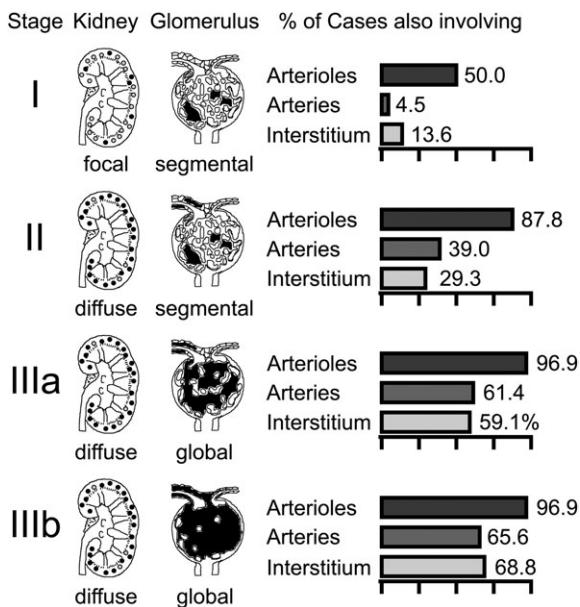**Fig. 2.** Dynamics of glomerular amyloid deposition (PAS, original magnification: ×400).

Fig. 3. Stages of glomerular amyloid deposition and involvement of other compartments.

case, a giant cell was noted adjacent to vascular amyloid (Figure 1N).

Interstitial pattern

The interstitial type was characterized by amyloid deposits surrounding the tubules, usually involving the tubular basement membranes, the peritubular capillaries and/or the vascular bundles of the vasa recta (Figure 1H and O). Most often, it was very prominent in the renal medulla and sometimes took a nodular form (Figure 1P). In most cases, the tubules were well preserved and did not show signs of tubular atrophy.

Additional involvement of the arterioles was present in most cases, of the arteries in ~50%. As in the vascular type, glomerular involvement was minimal in half of the cases and the remaining showed mild-to-moderate involvement.

Secondary changes in renal amyloidosis

The most frequent and important secondary changes due to amyloidosis were glomerular obsolescence, interstitial fibrosis with tubular atrophy and interstitial inflammation. The percentage of obsolescent glomeruli due to amyloid deposition increased with the number of glomeruli involved and a global rather than a segmental involvement (Figure 4A).

Interstitial fibrosis and tubular atrophy also increased with the amount of amyloid present (Figure 4B). In cases of either focal or diffuse segmental glomerular involvement, the extent was small (median 0%). Diffuse and late global involvement resulted in extensive interstitial fibrosis with tubular atrophy (median 60%, Kruskal–Wallis test: P < 0.0001). Interstitial inflammation in most cases was minimal and characterized by a lymphohistiocytic cellular infiltrate. Plasma cells, neutrophilic and eosinophilic granulocytes were not present. Other rare secondary changes noted were tubular or interstitial foam cells in 3% of the cases and giant cells adjacent to amyloid deposits in 2.5% of the cases.

Correlations between biochemical type, distribution patterns, secondary changes and clinical parameters

There was no correlation between the biochemical type of amyloid and amyloid distribution within the kidney (Figure 4C). However, AL amyloidosis was more often detected at an earlier stage than AA amyloidosis. One difference noted in the glomerular type was that AL amyloid was frequently present in the preglomerular arterioles even in cases with only minimal or mild glomerular involvement. In contrast, some cases of AA amyloidosis with moderate or severe glomerular involvement lacked deposits within the arterioles and/or arteries. In all cases of AL amyloidosis with a clinically reported monoclonal light chain, the specificity of the light chain found by immunohistochemistry was the same as the one found in the serum or urine.

The reported proteinuria at the time of biopsy was higher in the patients presenting with the glomerular type compared to the vascular type (Figure 5A). There was no significant difference compared to the interstitial type. Within the glomerular type, proteinuria significantly increased with diffuse involvement of the glomeruli (Figure 5B; median: focal segmental 5 g/day, diffuse segmental and diffuse global early 7 g/day and diffuse global late 9 g/day; Kruskal–Wallis test: P < 0.05).

Patients with the vascular type tended to present with a higher serum creatinine (Figure 5C). However, this was not significant. As expected, serum creatinine correlated with the area% of interstitial fibrosis with tubular atrophy (Spearman's r = 0.6585, P < 0.0001; Figure 5D). In relation to the pattern of glomerular amyloid deposition, creatinine was significantly increased once amyloid was distributed in a global fashion (Figure 5E; median: focal segmental 79 μmol/L, diffuse segmental 88 μmol/L, diffuse global early 121 μmol/L and diffuse global late 257 μmol/L; Kruskal–Wallis test: P < 0.0001).
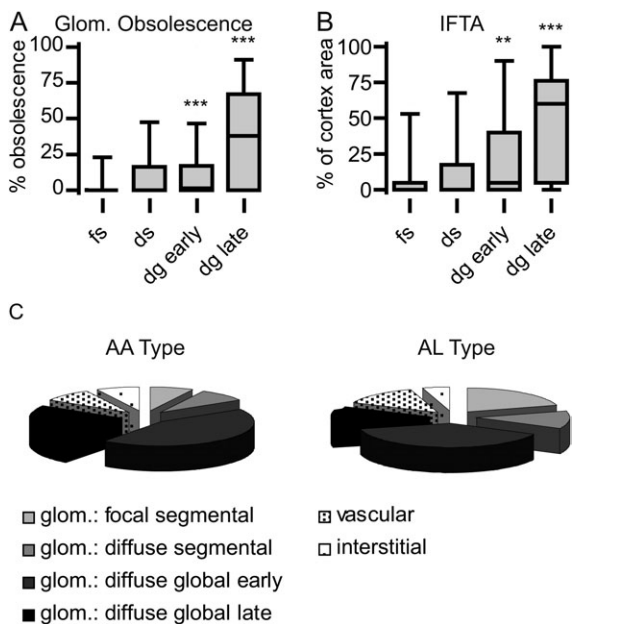
Fig. 4. Glomerular obsolescence (**A**) and amount of interstitial fibrosis with tubular atrophy (IFTA) (**B**) in different stages of glomerular amyloid deposition. Kruskal–Wallis test P <0.0001 for both A and B. Box plots show 25th, 50th and 75th percentile and the whiskers show the 5th and 95th percentile. fs, focal segmental; ds, diffuse segmental; dg, diffuse global. Levels of significance: **P < 0.01 and ***P < 0.001. (**C**) Percentage of cases with glomerular, vascular and interstitial distribution types in AA and AL amyloidosis. Glomerular type is further subdivided by stage.

Fig. 5. Correlation of morphological parameters with clinical data provided at the time of kidney biopsy. (**A**) Proteinuria plotted against amyloid distribution type. Kruskal–Wallis test, P < 0.0001. (**B**) Proteinuria plotted against glomerular stages. Kruskal–Wallis test, P < 0.05. (**C**) Serum creatinine plotted against amyloid distribution types. Kruskal–Wallis test, P = not significant. (**D**) Correlation between serum creatinine and interstitial fibrosis with tubular atrophy (IFTA). Spearman's $r = 0.6585$, P < 0.0001. (**E**) Serum creatinine plotted against glomerular stages. Kruskal–Wallis test, P < 0.0001. (A–C and E) Box plots show 25th, 50th and 75th percentile, the whiskers show the 5th and 95th percentile. fs, focal segmental; ds, diffuse segmental; dg, diffuse global. Levels of significance: *P < 0.05, **P < 0.01 and ***P < 0.001.

Discussion

Identification of amyloid and establishment of its biochemical type is the key information provided by the renal pathologists evaluating the patients' kidney biopsies. Using a systematic workup of standard histological sections and stains, we aimed to identify additional parameters which may be relevant to patient care, especially in the context of the emerging new anti-fibrillar therapies.

Undisputedly, immunohistochemical typing is currently the most important task in the workup of a renal biopsy with amyloidosis because it determines the clinical management and therapy [2, 13]. It should be performed in all cases. In the past, typing of AL amyloidosis using antisera against lambda and kappa light chains has been a major problem, often providing false-negative results [14–16]. We were fortunate to have amyloid-specific polyclonal sera against lambda and kappa light chains (kindly provided by Prof. R. Linke, Martinsried, Germany), which enabled us to reliably type >97% of our cases. These antisera have recently become commercially available. In the future, this will tremendously help pathologists typing AL amyloidosis, especially on paraffin sections. Our study also shows that as a first-step antisera against AA, AL lambda and AL kappa are sufficient to type the majority of cases.

Although the three amyloid distribution patterns have been described in the literature, they are frequently not mentioned in renal pathology textbooks and probably not reported by many pathologists [5, 6, 9]. It is hard to believe that the distribution patterns within the renal compartments
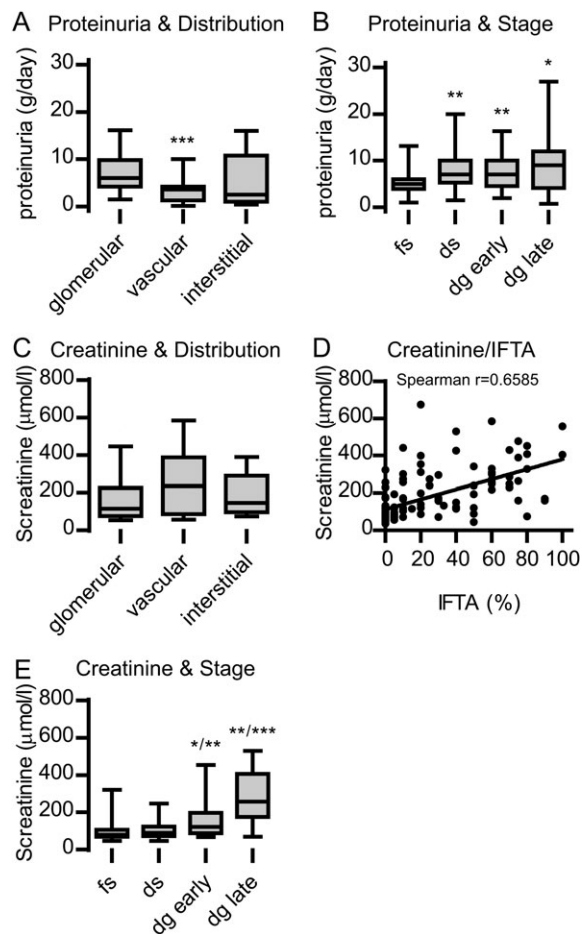
occur by mere chance. Both AL and AA may be dominantly deposited in any of the renal compartments, implying that these proteins are not a homogenous chemical entity. In recent years, much progress has been made in the understanding of the pathogenesis of amyloidosis [17–21]. The precise mechanism of amyloid deposition is not completely understood. However, once fibrils have been seeded, there is a strong tendency for further self-aggregation. In addition to the deposited fibrils, unstable precursor molecules may have a toxic effect resulting in further organ dysfunction [1]. Much evidence suggests that the chemicophysical properties of the amyloid fibrils determine their tropism in regard to which organs and also which compartments are affected [12, 22]. The chemicophysical properties in an individual case depend on the biochemical type, the amino acid sequence, especially in cases with mutations (AL, hereditary amyloidosis), and

proteolytic cleavage resulting in protein fragments of various sizes [10, 23, 24]. The latter has been described for both AA and ATTR proteins [10, 12]. Currently, the distribution patterns have only limited clinical meaning. This may change, once correlations have been established between certain chemicophysical properties and deposition patterns.

The glomerular pattern of amyloid deposition is most common, comprising >80% of the cases. Although glomerular amyloid deposition is clearly a continuous process, it can be arbitrarily divided into three stages: (I) focal segmental, (II) diffuse segmental and (III) diffuse global glomerular involvement. Stage III can be further divided into an early and a late phase. The stages correlate both with clinical as well as pathological parameters, making this staging useful and meaningful. Proteinuria is the clinical hallmark feature of glomerular amyloidosis, even in the early stage [9]. Proteinuria significantly increases with progression from a focal (I) to a diffuse (II and III) glomerular deposition. This is also true for the glomerular amyloid deposits in the vascular and interstitial distribution patterns. In contrast, a significant rise in serum creatinine was seen in the transition from segmental (I and II) to global lesions (III) with a further increase in the late global stage. This is most likely due to the secondary interstitial fibrosis and tubular atrophy, which shows a strong correlation with the glomerular stages. The high correlation between serum creatinine and interstitial fibrosis, which was also found in this study, is well known and has already been shown for renal amyloidosis >20 years ago [4, 9, 25]. In both AL and AA amyloidosis, the majority of patients are diagnosed in Stage III. It is important to point out that these later stages have increasing chronic lesions (glomerular obsolescence, tubular atrophy and interstitial fibrosis), which may not be accessible to anti-amyloid therapy. Our series contained only few cases with other glomerular patterns such as the nodular type [26] and there was no correlation with the biochemical amyloid type.

Recently, Sen and Sarsik [27] proposed a histopathologic classification, scoring and grading system for renal amyloidosis similar to the classification of systemic lupus erythematodes. The staging system used by us is similar in several ways but in our opinion much easier to use in the setting of daily routine diagnostics. In addition, we show clear correlations with pathological features (glomerular obsolescence and interstitial fibrosis with tubular atrophy) and laboratory parameters (proteinuria and serum creatinine).

Depending on the stage, we noticed an increasingly less conspicuous involvement of preglomerular arterioles, interlobular arteries and the interstitium. It is not clear whether this reflects an 'overflow' mechanism or is due to a different fibril composition.

The vascular pattern is characterized by dominant amyloid deposits within arteries and arterioles. The deposition within the blood vessels was quite heterogenous in regard to segmental or circular deposits and also intima or media involvement. A number of previous studies have described the vascular in comparison to the glomerular form [5–9]. The frequency of the vascular distribution pattern varied between 12.5 and 39%, and it was 9.4% in our series. As in the other studies, proteinuria in the vascular pattern was lower. It is believed that the vascular pattern frequently presents with renal insufficiency. In this regard, our data showed only a nonsignificant trend. This may be due to the high number of glomerular cases diagnosed late in the course of the disease.

The interstitial pattern accounts for only 5.9% of our cases. Amyloid deposits either surround the tubules and peritubular capillaries of the cortex or may predominantly affect the blood vessels along the vasa recta. In renal biopsies, it is difficult to tell the distribution within medulla and cortex, but the amyloid deposits may be limited to the medulla [5, 28]. Some of the cases documented in the literature have presented as diabetes insipidus renalis [29, 30]. None of our cases showed this presentation.

Our series contains only one case with a hereditary amyloidosis and we did not identify cases with other infrequent amyloid types. We have not tested for the newly described leukocyte cell-derived chemotoxin 2 protein [31, 32]. Therefore, we cannot tell whether these infrequent amyloid types show any preferential deposition patterns.

Several drugs are being developed that target the formation and stability of amyloid fibrils or the conversion of precursor proteins to folding intermediates [33–36] that will likely change amyloidosis treatment. It is well conceivable that not only the formation of new renal amyloid deposits will be blocked but also that existing amyloid deposits may be degraded. Looking at the distribution of amyloid within the renal compartments and particularly the stage of glomerular deposition, one would expect that the late stages, IIIa and, especially, IIIb, may not respond very well to anti-fibrillar therapy due to the chronic glomerular and tubulointerstitial lesions. One will also have to consider what will happen to the advanced glomerular or vascular lesions once the amyloid is taken away, especially if the resident cells have mostly disappeared. We believe that it is likely that eventually some type of scar (i.e. glomerular and/or vascular sclerosis) will evolve. We therefore think that in the future, the amyloid distribution pattern, the glomerular stage and the amount of interstitial fibrosis with tubular atrophy will become important parameters for clinical decision making in patients with renal amyloidosis.

In summary, our findings show three easily recognizable distribution patterns of amyloid deposition in the kidney. These do not correlate with the biochemical type but may become relevant for future correlations with physicochemical properties of amyloid and anti-fibrillar therapies. Staging amyloidosis and providing a good estimate of the amount of interstitial fibrosis with tubular atrophy may be useful to predict the efficacy of an anti-fibrillar treatment.

References

1. Dember LM. Amyloidosis-associated kidney disease. *J Am Soc Nephrol* 2006; 17: 3458–3471
2. Linke RP, Oos R, Wiegel NM *et al.* Classification of amyloidosis: misdiagnosing by way of incomplete immunohistochemistry and how to prevent it. *Acta Histochem* 2006; 108: 197–208

3. von Hutten H, Mihatsch M, Lobeck H *et al.* Prevalence and origin of amyloid in kidney biopsies. *Am J Surg Pathol* 2009; 33: 1198–1205

4. Bergesio F, Ciciani AM, Manganaro M *et al.* Renal involvement in systemic amyloidosis: an Italian collaborative study on survival and renal outcome. *Nephrol Dial Transplant* 2008; 23: 941–951

5. Westermark P, Sletten K, Eriksson M. Morphologic and chemical variation of the kidney lesions in amyloidosis secondary to rheumatoid arthritis. *Lab Invest* 1979; 41: 427–431

6. Falck HM, Törnroth T, Wegelius O. Predominantly vascular amyloid deposition in the kidney in patients with minimal or no proteinuria. *Clin Nephrol* 1983; 19: 137–142

7. Looi L, Cheah P. Histomorphological patterns of renal amyloidosis: a correlation between histology and chemical type of amyloidosis. *Hum Pathol* 1997; 28: 847–849

8. Uda H, Yokota A, Kobayashi K *et al.* Two distinct clinical courses of renal involvement in rheumatoid patients with AA amyloidosis. *J Rheumatol* 2006; 33: 1482–1487

9. Verine J, Mourad N, Desseaux K *et al.* Clinical and histological characteristics of renal AA amyloidosis: a retrospective study of 68 cases with a special interest to amyloid-associated inflammatory response. *Hum Pathol* 2007; 38: 1798–1809

10. Westermark GT, Sletten K, Grubb A *et al.* AA-amyloidosis. Tissue component-specific association of various protein AA subspecies and evidence of a fourth SAA gene product. *Am J Pathol* 1990; 137: 377–383

11. Comenzo RL, Zhang Y, Martinez C *et al.* The tropism of organ involvement in primary systemic amyloidosis: contributions of Ig V(L) germ line gene use and clonal plasma cell burden. *Blood* 2001; 98: 714–720

12. Ihse E, Ybo A, Suhr O *et al.* Amyloid fibril composition is related to the phenotype of hereditary transthyretin V30M amyloidosis. *J Pathol* 2008; 216: 253–261

13. Picken MM. Immunoglobulin light and heavy chain amyloidosis AL/AH: renal pathology and differential diagnosis. *Contrib Nephrol* 2007; 153: 135–155

14. Satoskar AA, Burdge K, Cowden DJ *et al.* Typing of amyloidosis in renal biopsies: diagnostic pitfalls. *Arch Pathol Lab Med* 2007; 131: 917–922

15. Picken MM. New insights into systemic amyloidosis: the importance of diagnosis of specific type. *Curr Opin Nephrol Hypertens* 2007; 16: 196–203

16. Solomon A, Murphy CL, Westermark P. Unreliability of immunohistochemistry for typing amyloid deposits. *Arch Pathol Lab Med* 2008; 132: 14

17. Westermark P. Aspects on human amyloid forms and their fibril polypeptides. *FEBS J* 2005; 272: 5942–5949

18. Westermark P. The pathogenesis of amyloidosis: understanding general principles. *Am J Pathol* 1998; 152: 1125–1127

19. Pepys MB. Amyloidosis. *Annu Rev Med* 2006; 57: 223–241

20. Page LJ, Suk JY, Bazhenova L *et al.* Secretion of amyloidogenic gelsolin progressively compromises protein homeostasis leading to the intracellular aggregation of proteins. *Proc Natl Acad Sci USA* 2009; 106: 11125–11130

21. Elimova E, Kisilevsky R, Ancsin JB. Heparan sulfate promotes the aggregation of HDL-associated serum amyloid A: evidence for a proamyloidogenic histidine molecular switch. *FASEB J* 2009; 23: 3436–3448

22. Pepys MB. A molecular correlate of clinicopathology in transthyretin amyloidosis. *J Pathol* 2009; 217: 1–3

23. Westermark GT, Sletten K, Westermark P. Massive vascular AA-amyloidosis: a histologically and biochemically distinctive subtype of reactive systemic amyloidosis. *Scand J Immunol* 1989; 30: 605–613

24. Bergström J, Gustavsson A, Hellman U *et al.* Amyloid deposits in transthyretin-derived amyloidosis: cleaved transthyretin is associated with distinct amyloid morphology. *J Pathol* 2005; 206: 224–232

25. Bohle A, Wehrmann M, Eissele R *et al.* The long-term prognosis of AA and AL renal amyloidosis and the pathogenesis of chronic renal failure in renal amyloidosis. *Pathol Res Pract* 1993; 189: 316–331

26. Shiiki H, Shimokama T, Yoshikawa Y *et al.* Renal amyloidosis. Correlations between morphology, chemical types of amyloid protein and clinical features. *Virchows Arch A Pathol Anat Histopathol* 1988; 412: 197–204

27. Sen S, Sarsik B. A proposed histopathologic classification, scoring, and grading system for renal amyloidosis. *Arch Pathol Lab Med* 2010; 134: 532–544

28. Gregorini G, Izzi C, Obici L *et al.* Renal apolipoprotein A-I amyloidosis: a rare and usually ignored cause of hereditary tubulointerstitial nephritis. *J Am Soc Nephrol* 2005; 16: 3680–3686

29. Carone FA, Epstein FH. Nephrogenic diabetes insipidus caused by amyloid disease. Evidence in man of the role of the collecting ducts in concentrating urine. *Am J Med* 1960; 29: 539–544

30. Asmundsson P, Snaedal J. Persistent water diuresis in renal amyloidosis. A case report. *Scand J Urol Nephrol* 1981; 15: 77–79

31. Benson MD, James S, Scott K *et al.* Leukocyte chemotactic factor 2: a novel renal amyloid protein. *Kidney Int* 2008; 74: 218–222

32. Larsen CP, Walker PD, Weiss DT *et al.* Prevalence and morphology of leukocyte chemotactic factor 2-associated amyloid in renal biopsies. *Kidney Int* 2010; 77: 816–819

33. Hrncic R, Wall J, Wolfenbarger DA *et al.* Antibody-mediated resolution of light chain-associated amyloid deposits. *Am J Pathol* 2000; 157: 1239–1246

34. O'Nuallain B, Hrncic R, Wall JS *et al.* Diagnostic and therapeutic potential of amyloid-reactive IgG antibodies contained in human sera. *J Immunol* 2006; 176: 7071–7078

35. Dember LM, Hawkins PN, Hazenberg BPC *et al.* Eprodisate for the treatment of renal disease in AA amyloidosis. *N Engl J Med* 2007; 356: 2349–2360

36. O'Nuallain B, Allen A, Kennel SJ *et al.* Localization of a conformational epitope common to non-native and fibrillar immunoglobulin light chains. *Biochemistry* 2007; 46: 1240–1247